Thermodynamics of Cu^{2+} Adsorption on soil Humin

Li, C.L. [1], Wang, S. [2], Ji, F. [1], Zhang, J.J. [1*] and Wang, L.C. [3]

[1] College of Resource and Environmental Science, Jilin Agricultural University, Changchun, 130118,P.R. China

[2] College of Plant Science, Jilin Agricultural Science and Technology College, Jilin, 132101, P.R. China

[3] Institute of Agricultural Resources and Environments, Jilin Academy of Agricultural Sciences, Changchun, 130124, P.R. China

ABSTRACT: The adsorption thermodynamic characteristic of Cu^{2+} from aqueous solution onto humin and also humic acid from a typical black soil in northeast China were examined at three different temperatures (298, 318 and 338 K) by batch isotherm experiments. Results showed that humin was structurally different from humic acid. The increase of temperature had a positive effect on the adsorption process. Freundlich equation described the equilibrium data better with respect to Langmuir equation. Thermodynamic parameters, i.e. standard free energy changes (ΔG^o), standard enthalpy change (ΔH^o) and standard entropy change (ΔS^o), revealed that Cu^{2+} adsorption by humin and humic acid were a feasible, spontaneous and endothermic process with an increase in disorder. The values of isosteric heat of adsorption (ΔH_x) increased with increasing surface Cu^{2+} loading, and the increase in ΔH_x values was smaller for humin than for humic acid. The results indicated that humin and humic acid possessed energetically heterogeneous surfaces. Humic acid had greater surface heterogeneity than humin

Key words: Humin, Humic acid, Cu^{2+}, Adsorption isotherm, Thermodynamic parameters

INTRODUCTION

Soil organic matter is one of the most important soil components. It has a profound effect on the physical, chemical and biological functions of soil, including aggregate stability, water-holding capacity, cation exchange capacity, nutrient retention and release, etc. (Krull *et al.*, 2004). Humic substances represent the largest constituent (60-80%) of soil organic matter, responsible for many complex chemical reactions in soil such as adsorption, ion exchange, complexation, redox, dissolution, and precipitate (Stevenson, 1994; Schnitzer, 1999). Generally, humic substances can be divided into three main fractions based on the basis of their solubility in aqueous solution at different pH values: humic acid, which is not soluble in water at pH<2 but is soluble at less acidic pH values; fulvic acid, which is soluble in water at all pH values; and humin, which is not soluble in water at any pH value (Aiken *et al.*, 1985; Stevenson, 1994). One of the most striking features of humic substances is their strong interaction with inorganic and organic pollutants (Perminova *et al.*, 2005). The adsorption of metal ions on humic substances has long

been known to play an important role in controlling the behavior and fate of trace metals in the environment. The majority of studies published to date have focused on the adsorption characteristics of metal ions on base-soluble fractions of humic substances, namely humic and fulvic acids. However, very little information is available on humin. Only a few have reported on the adsorption properties of metal ions on humin from peat (Contreras *et al.*, 2006; De la Rosa *et al.*, 2003; Gardea-Torresdey *et al.*, 1996), lignite (Havelcová *et al.*, 2009), and brown coal (Alvarez-Puebla *et al.*, 2005; Alvarez-Puebla *et al.*, 2006). In addition, Helal *et al.* (1998, 2006a, 2006b) and Rigol *et al.* (1998) reported the adsorption features of some radionuclides (^{134}Cs, ^{137}Cs, ^{90}Sr, ^{153}Gd, ^{110m}Ag, ^{60}Co and ^{65}Zn) on humin from peat soil or agricultural soil.

Copper (Cu) is an essential trace element for plant nutrition, while it could become toxic when its concentration is high in the soil. In our previous study, we determined, for the first time, the adsorption isotherm of Cu^{2+} on humin isolated from a forest soil

*Corresponding author E-mail: zhangjinjing@126.com

using batch equilibration method (Zhang *et al.*, 2012). However, the thermodynamic properties of the adsorption of Cu^{2+} on soil humin, which can provide useful information for evaluating the mechanisms of adsorption process, are still lacking. On the other hand, the interaction of humin with metal ions is closely related to their chemical structures. Elemental analysis and solid-state ^{13}C cross-polarization magic angle spinning nuclear magnetic resonance (^{13}C CPMAS NMR) spectroscopy are powerful tools for elucidating the structural characteristics of humin (Rice and MacCarthy, 1991; Simpson *et al.*, 2011). The black soil is important for its high level of fertility and productivity. Black soil region in northeast China is one of the three major black lands in the world. The main objective of the present study are to evaluate the thermodynamics of Cu^{2+} adsorption on humin from a typical black soil in northeast China at different temperatures (298, 318 and 338 K) by conducting batch isotherm experiments. Moreover, the isolated humin are characterized using elemental analysis and solid-state ^{13}C CPMAS NMR spectroscopy. The differences of structural and Cu^{2+} adsorption characteristics between humin and humic acid are also compared.

MATERIALS & METHODS

The soil used in the study is black soil (Haplic haeozem according to the FAO Soil Classification, and Typic Hapludoll according to the USDA Soil Taxonomy). The surface soil (0-20 cm) samples were collected from a cultivated maize field located at Changchun City (43º482 443 N, 125º232 453 E, 230.7 m above sea level), Jilin Province, Northeast China. The collected soil samples were air-dried, milled and sieved through a 2 mm sieve. Selected physical and chemical properties of the soil were analyzed using the procedure recommended (Lao, 1988), and the results are presented in Table 1. The extraction, fractionation and purification of humic acid and humin were performed following the procedure described by Zhang *et al.* (2009b, 2011a). Briefly, 100 g of each soil sample was first suspended in distilled water and dilute HCl to remove poorly decomposed light fractions and carbonates, respectively. The soil residue was then extracted with a solution of 0.1 mol L^{-1} NaOH and 0.1 mol L^{-1} $Na_4P_2O_7$ using a 1:10 sample:extractant ratio at room temperature. The extraction procedure was repeated 25 times until the supernatant was almost colorless. The combined

alkaline supernatant was acidified to pH 1.0 with 6 mol L^{-1} HCl to separate the humic acid fraction. The insoluble solid residue remaining after alkaline extraction was referred to as humin fraction. The humic acid fraction was purified by de-ashing with 0.5% HCl-HF solution after three cycles of dissolution in 0.1 mol L^{-1} NaOH and reprecipitation with 6 mol L^{-1} HCl. The humin fraction was purified by de-ashing with 20% HCl-HF solution. The humic acid and humin samples were then further purified by dialyzing against distilled water until they were Cl⁻-free. Finally, the purified humic acid and humin were freeze-dried, ground to <0.1 mm and stored in a desiccator for further use.

The C, H, N, and S contents were determined using an Elementar Vario MICRO elemental analyzer (Germany), and the O content was calculated by mass difference. The ash contents were measured by thermogravimetric analysis performed with a Shimadzu DTG-60 thermal analyzer (Japan) from room temperature to 750 ºC at a heating rate of 10 ºC min⁻¹. Solid-state ^{13}C cross-polarization magic angle spinning nuclear magnetic resonance (^{13}C CPMAS NMR) spectra were obtained using a Bruker AVANCE III 400 WB spectrometer (Switzerland) operating at 100.6 MHz. The operating conditions were as follows: spinning rate 12 kHz, contact time 2 ms, and recycle time 6 s. The spectra were divided into four main chemical shift regions: alkyl C (0-50 ppm), O-alkyl C (50-110 ppm), aromatic C (110-160 ppm), and carbonyl C (160-200 ppm). The total range of O-alkyl C was further divided into regions of methoxyl C (50-60 ppm) and carbohydrate C (60-110 ppm), and the total range of aromatic C into regions of aryl C (110-145 ppm) and phenolic C (145-160 ppm) (Zhang *et al.*, 2011a). The relative intensity of each chemical shift region was determined using the integration routine of the spectrometer. The correction of spinning side band (SSB) was made according to Conte *et al.* (1997).

The adsorption experiments were carried out under ambient conditions by using batch technique. The solid adsorbents (humic acid and humin), $NaNO_3$ background electrolyte solution and $Cu(NO_3)_2$ stock solution were added into 50 mL polyethylene centrifuge tubes to achieve the desired concentrations of different components (i.e. adsorbent dosage 0.2 g L^{-1}, ion strength 0.01 mol L^{-1} $NaNO_3$, initial Cu^{2+} concentration 0-80 mg L^{-1}). The initial pH of the solution was adjusted to 5.5 with 0.1 mol L^{-1} HNO_3 and 0.1 mol L^{-1} NaOH, but no further

Table 1. Selected properties of the soil used in the experiment

Organic C (g kg⁻¹)	Total N (g kg⁻¹)	Total P (g kg⁻¹)	pH	Sand (20-2000 μm) (g kg⁻¹)	Silt (2-20 μm) (g kg⁻¹)	Clay (<2 μm) (g kg⁻¹)
11.2	1.33	0.47	6.50	472.3	256.2	271.5

pH adjustment was conducted during the adsorption process. The suspensions were shaken at a constant speed of 140 rpm in a shaking water bath with temperature 298, 318 and 338 K, respectively. After shaking the tubes for 24 h, the solid and liquid phases were separated by centrifugation at 16000 rpm for 15 min. The solution was then filtered, and the filtrate was analyzed for Cu^{2+} concentration using TAS-990 atomic absorption spectrometry (China). All experimental data were the average of duplicate or triplicate determination.

The amounts of adsorbed Cu^{2+} were calculated by the mass balance equation [Eq. (1)]:

$$q_e = (C_0 - C_e)\frac{V}{m} \tag{1}$$

where q_e is the amount of Cu^{2+} adsorbed at equilibrium (mg g^{-1}), C_0 is the initial Cu^{2+} concentration (mg L^{-1}), C_e is the equilibrium Cu^{2+} concentration in solution (mg L^{-1}), V is the volume of the solution (L), m is the mass of the adsorbents (g).

The adsorption isotherm data were fitted using the Langmuir model [Eqs. (2) and (3)] and the Freundlich model [Eqs. (4) and (5)]:

$$q_e = \frac{k_1 q_m C_e}{1 + k_1 C_e} \qquad \text{(non-linear form)} \tag{2}$$

$$\frac{C_e}{q_e} = \frac{C_e}{q_m} + \frac{1}{q_m k_1} \quad \text{(linear form)} \tag{3}$$

$$q_e = k_2 C_e^{1/n} \quad \text{(non-linear form)} \tag{4}$$

$$\ln q_e = \frac{1}{n}\ln C_e + \ln k_2 \quad \text{(linear form)} \tag{5}$$

where q_m and k_1 are the Langmuir constants related to the maximum adsorption capacity (mg g^{-1}) and adsorption energy (L mg^{-1}), respectively; k_2 and n are the Freundlich constants represent the adsorption capacity (mg g^{-1} (mg L^{-1})$^{-1/n}$) and adsorption intensity, respectively.

The thermodynamic parameters of adsorption, i.e., the standard free energy changes (ΔG°, kJ mol^{-1}), the standard enthalpy change (ΔH°, kJ mol^{-1}) and the standard entropy change (ΔS°, J mol^{-1} K^{-1}), were

calculated from the temperature dependent adsorption isotherms using classical thermodynamic equations [Eqs. (6)-(8)] (Mahmoodi *et al.*, 2011; Sheng *et al.*, 2009):

$$K_d = \frac{C_0 - C_e}{C_e}\frac{V}{m} \tag{6}$$

$$\ln K_d = \frac{\Delta S^\circ}{R} - \frac{\Delta H^\circ}{RT} \tag{7}$$

$$\Delta G^\circ = \Delta H^\circ - T\Delta S^\circ \tag{8}$$

where K_d is the thermodynamic equilibrium constant (mL g^{-1}), R is the ideal gas constant (8.314 J mol^{-1} K^{-1}), T is the reaction temperature (K). The values of ΔH° and ΔS° are obtained from the slope and y-intercept of the plot of ln K_d versus $1/T$.

The isosteric heat of adsorption (ΔH_x, kJ mol^{-1}) at constant surface loading (q_e=2, 4, 6, 8, 10, 12, 14, 16 mg g^{-1}) was calculated using the Clausius-Clapeyron equation [Eq. (9)] (Anirudhan and Radhakrishnan, 2011):

$$\frac{d(\ln C_e)}{dT} = -\frac{\Delta H_x}{RT^2} \tag{9}$$

where C_e (mg L^{-1}) is the equilibrium Cu^{2+} concentration at constant q_e (mg g^{-1}), which was obtained from the adsorption isotherm data at various temperatures T (K). The ΔH_x values were calculated from the slope resulting from plotting of ln C_e versus $1/T$.

RESULTS & DISCUSSION

The elemental composition and atomic ratios of humic acid and humin are presented in Table 2. Compared with humic acid, humin contained more C, H and S and less N and O. The H/C ratio was lower whereas the O/C ratio was higher for humic acid than for humin, indicating that humin was more aliphatic and less polar (Xing *et al.*, 2005). Meanwhile, the C/N ratio of humic acid was lower than that of humin, suggesting that resistant forms of N were depleted in humin during the humification process (Zhang *et al.*, 2011b).

The ^{13}C CPMAS NMR spectra of humic acid and humin are shown in Fig. 1. The spectra exhibited major

Table 2. Elemental composition and atomic ratios of humic acid and humin from black soil

Samples	C [a] (g kg^{-1})	H [a] (g kg^{-1})	N [a] (g kg^{-1})	S [a] (g kg^{-1})	O [a] (g kg^{-1})	H/C (atomic ratio)	O/C (atomic ratio)	C/N (atomic ratio)
Humic acid	575.4	39.0	37.0	4.11	344.5	0.813	0.449	18.1
Humin	638.1	52.1	19.1	5.13	285.2	0.981	0.335	38.3

[a] On a ash-free basis.

Table 3. Relative carbon distribution (%) in different regions of chemical shift in ¹³C CPMAS NMR spectra of humic acid and humin from black soil

Samples	Chemical shift regions (ppm)								A/ O-A[a]	Alip/ Arom[b]	HB/ HI[c]
	0-50	50-60	60-110	0-110	110-145	145-160	110-160	160-200			
Humic acid	21.9	6.45	18.5	46.9	23.2	3.23	26.5	26.9	0.88	1.77	0.93
Humin	34.7	2.57	17.5	54.8	19.8	2.37	22.2	23.1	1.74	2.47	1.32

[a] alkyl C/O-alkyl C = (0-50)/(50-110).
[b] aliphatic C/aromatic C = [(0-50)+(50-110)]/(110-160).
[c] hydrophobic C/hydrophilic C = [(0-50)+(110-160)]/[(50-110)+(160-200)].
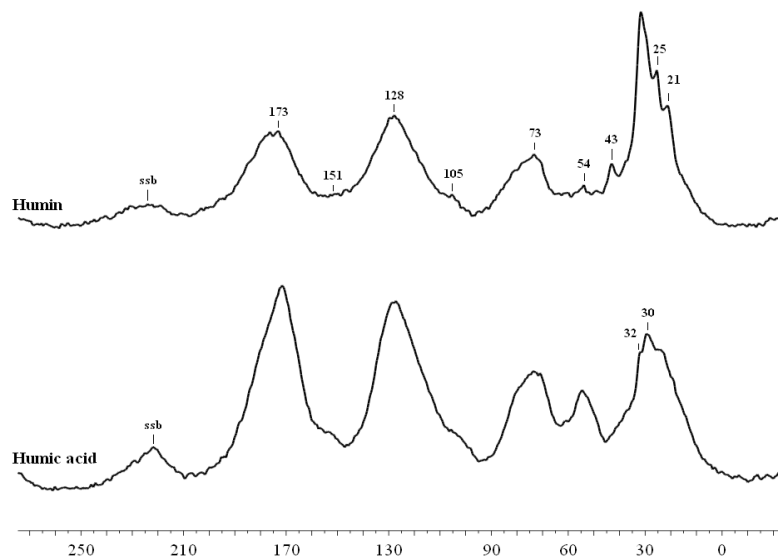
Fig. 1. ¹³C CPMAS NMR spectra of humic acid and humin from black soil

signal peaks at 21, 25, 30, 32, 43, 54, 73, 105, 128, 151 and 173 ppm. Based on Zhang *et al.* (2009b; 2011a), the peaks at 21, 25, 30, 32 and 43 ppm in the alkyl C region were assigned as $-CH_3$, $-CH_2$-, amorphous $-(CH_2)_n$-, crystalline $-(CH_2)_n$-, and branched aliphatic C, respectively. The signals at 54, 73 and 105 ppm in the O-alkyl C region were ascribed to methoxyl C in lignin, and -CHOH-, and anomeric C in carbohydrate, respectively. The signals at 128 and 151 ppm in the aromatic C region represented C- and H-substituted, and O-substituted aromatic C from lignin, respectively. The signal at 173 ppm in the carbonyl C region was indicative of carboxylic acid, amide and ester. Moreover, a distinct peak appeared in the range of 222–224 ppm was assigned as spinning side band (SSB).

The relative intensities of C functional groups of humic acid and humin are presented in Table 3. Across the two humic substance fractions, the intensity of aliphatic C (the sum of alkyl C and O-alkyl C, 46.9%-54.8%) was higher than that of aromatic C (22.2%-26.5%) and carbonyl C (23.1%-26.9%). Moreover,

carbohydrate C showed the highest intensity (17.5%-18.5%) in the O-alkyl C region, and the intensity of aryl C (19.8%-23.2%) was the highest in the aromatic C region. Compared with humic acid, humin contained larger proportions of alkyl C, but smaller proportions of methoxyl C, carbohydrate C, aryl C, phenolic C and carbonyl C. The ratios of alkyl C/O-alkyl C, aliphatic C/aromatic C and hydrophobic C/hydrophilic C of humin were higher than those of humic acid. The ratios of alkyl C/O-alkyl C, aliphatic C/aromatic C and hydrophobic C/hydrophilic C have been used as indices of the degrees of humification, aliphaticity and hydrophobicity of humic substances, respectively. Larger values of the ratios indicate that humic substances are more humified, aliphatic and hydrophobic (Zhang *et al.*, 2011a). Furthermore, alkyl C/O-alkyl C ratio is generally considered a more suitable index for describing the humification degree of humic substance fractions with respect to other indices such as aromaticity (Chen and Chiu, 2003; Mathers and Xu, 2003). Thus, our results implied that humin was the more humified, aliphatic and hydrophobic compared
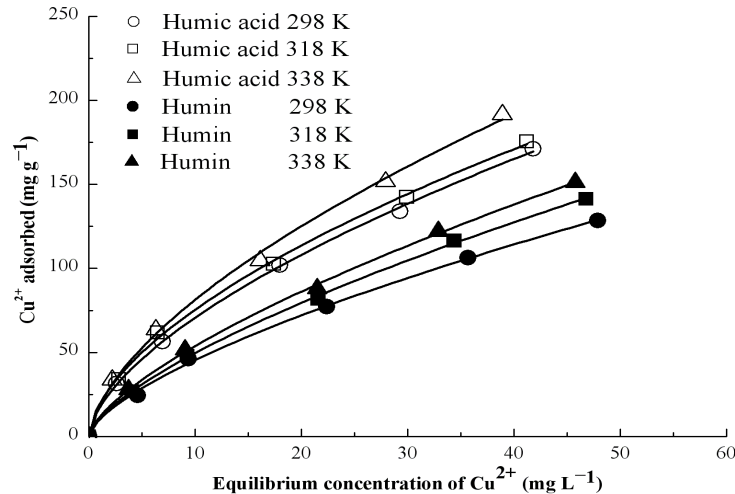
Fig. 2. Cu²⁺ adsorption isotherms of humic acid and humin from black soil at different temperatures. Symbols denote experimental data, and lines represent the model fitting of Freundlich equation
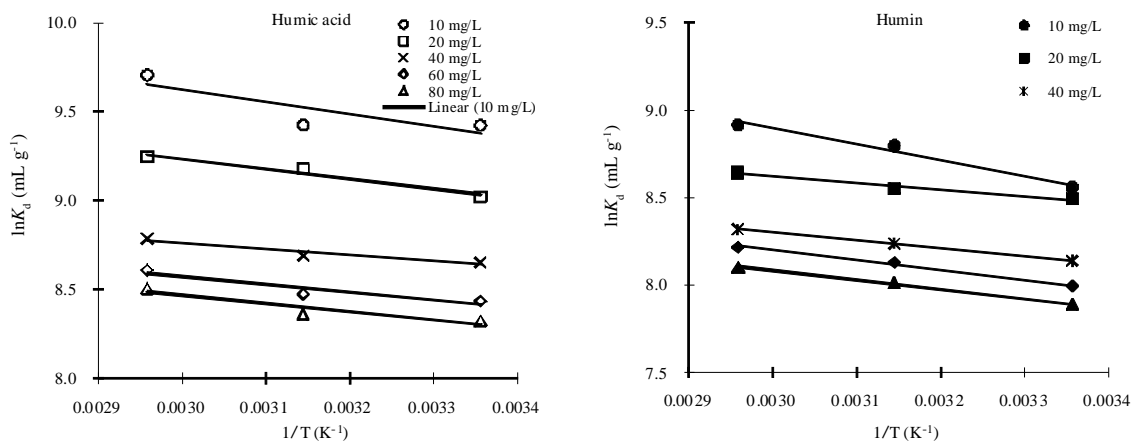
Fig. 3. Linear plot of ln K_d vs. 1/T for Cu²⁺ adsorption on humic acid and humin from black soil

with corresponding humic acid. The result of aliphatic C/aromatic C ratio was in accordance with that of H/C ratio.

The adsorption isotherms of Cu²⁺ on humic acid and humin at three different temperatures are shown in Fig. 2. It could be seen that the amounts of adsorbed Cu²⁺ on the two humic substance fractions increased with increasing Cu²⁺ concentration. On the other hand, the amounts of Cu²⁺ adsorbed on the two adsorbents also increased with rising temperature, indicating that the adsorption of Cu²⁺ was promoted at higher temperature. The possible interpretation for the promotion of Cu²⁺ adsorption at higher temperature is that the adsorption of well hydrated Cu²⁺ on humic acid and humin is an endothermic process in essence (Li *et al.*, 2011; Sheng *et al.*, 2009). Compared with humic acid, the adsorption

amounts of humin for Cu²⁺ were lower. The adsorption percentages of Cu²⁺ ranged from 47.7% to 79.2% for humic acid and from 40.1% to 62.5% for humin. The parameters of linearized Langmuir and Freundlich equations obtained by fitting the isotherms are given in Table 4. The adsorption data could be well described by both Langmuir and Freundlich equations with coefficient of determination (R^2) greater than 0.925. However, the Freundlich equation gave a better fit with R^2 values ranging from 0.993 to 1.000. Based on the Langmuir equation, the maximum adsorption capacities of Cu²⁺ (q_m) on humic acid and humin were 243.9 and 227.3 mg g⁻¹ at 298 K, respectively. The higher adsorption capacities of humic acid to Cu²⁺ was confirmed by the larger values of the Langmuir constant k_1 and the Freundlich constant k_2 for humic acid than for humin. The *n* values in the Freundlich equation were larger than 1, indicating a favorable and

Table 4. Adsorption isotherm parameters derived from linear Langmuir and Freundlich equations for Cu²⁺ adsorption on humic acid and humin from black soil at three different temperatures

Samples	T (K)	Langmuir			Freundlich		
		$q_m{}^a$	$k_1{}^b$	R^{2e}	n^c	$k_2{}^d$	R^{2e}
Humic acid							
	298	243.9	0.047	0.953	1.667	18.07	1.000
	318	250.0	0.050	0.962	1.699	19.64	0.997
	338	270.3	0.052	0.925	1.718	22.00	0.998
Humin							
	298	227.3	0.025	0.975	1.433	8.791	0.993
	318	243.9	0.027	0.952	1.475	10.43	0.999
	338	256.4	0.028	0.946	1.488	11.51	0.999

[a] q_m: Maximum adsorption quantity (mg g⁻¹). - [b] k_1: Langmuir constants (L mg⁻¹). - [c] n: Freundlich constants (dimensionless). [d] k_2: Freundlich constants (mg g⁻¹ (mg L⁻¹)⁻¹ᐟⁿ). - [e] R^2: Coefficient of determination.

Table 5. Values of thermodynamic parameters for the adsorption of Cu²⁺ on humic acid and humin from black soil.

Samples	C_0 (mg L⁻¹)	ΔH^o (kJ mol⁻¹)	ΔS^o (J mol⁻¹ K⁻¹)	ΔG^o (kJ mol⁻¹)		
				298 K	318 K	338 K
Humic acid						
	10	5.80	97.4	-23.2	-25.2	-27.1
	20	4.70	90.0	-22.4	-24.2	-26.0
	40	2.81	81.3	-21.4	-23.0	-24.7
	60	3.60	82.1	-20.9	-22.5	-24.1
	80	3.81	81.8	-20.6	-22.2	-23.8
Humin						
	10	7.50	96.4	-21.2	-23.2	-25.1
	20	3.06	80.9	-21.0	-22.6	-24.3
	40	3.71	80.1	-20.2	-21.8	-23.4
	60	4.68	82.2	-19.8	-21.5	-23.1
	80	4.43	80.5	-19.6	-21.2	-22.8

heterogeneous adsorption of Cu²⁺ on the two fractions of humic substances (Zhang *et al.*, 2009a). The degree of adsorption favorability and heterogeneity was higher for humic acid than for humin, which was also consistent with the larger Cu²⁺ adsorption of the former. The greater amounts of Cu²⁺ adsorption on humic acid than on humin could be attributed to the higher carboxyl and phenolic hydroxyl groups of the former (Table 3). On the other hand, the Langmuir and Freundlich isotherm parameters all increased with the increase in temperature, which agreed with the promotion of Cu²⁺ adsorption at higher temperature. The thermodynamic parameters calculated from Eqs. (6) to (8) are listed in Table 6, and the relevant plot of ln K_d vs. $1/T$ is given in Fig. 3. The magnitude of ΔG^o, ΔH^o, and ΔS^o values ranged from -20.6 kJ mol⁻¹, 3.81 kJ mol⁻¹, 81.3 J mol⁻¹ K⁻¹ to -27.1 kJ mol⁻¹, 5.80 kJ mol⁻¹, 97.4 J mol⁻¹ K⁻¹ for humic acid, and from -19.6 kJ mol⁻¹, 4.43 kJ mol⁻¹, 80.1 J mol⁻¹ K⁻¹ to -25.1 kJ mol⁻¹, 7.50 kJ

mol⁻¹, 96.4 J mol⁻¹ K⁻¹ for humin, respectively. The negative ΔG^o values at all temperatures indicated the feasibility and spontaneous nature of the adsorption of Cu²⁺ on humic acid and humin, which means that the adsorptive force is strong enough to break the potential and lead the reaction to bind Cu²⁺ onto the surface functional groups of humic substance fractions (Li *et al.*, 2008). The decrease in ΔG^o values with increase in temperature implied that the adsorption process was more favorable at higher temperature. The positive ΔH^o values indicated that the adsorption reaction was an endothermic process, which is supported by the results that the adsorption of Cu²⁺ on humic acid and humin increased with increasing temperature. The positive ΔS^o values reflected the affinity of the humic substance fractions towards Cu²⁺ and the increase of the degree of freedom at the solid/liquid interface during the adsorption process. In the study of Prado and Airoldi (2003), they showed that the adsorption of Cu²⁺ on
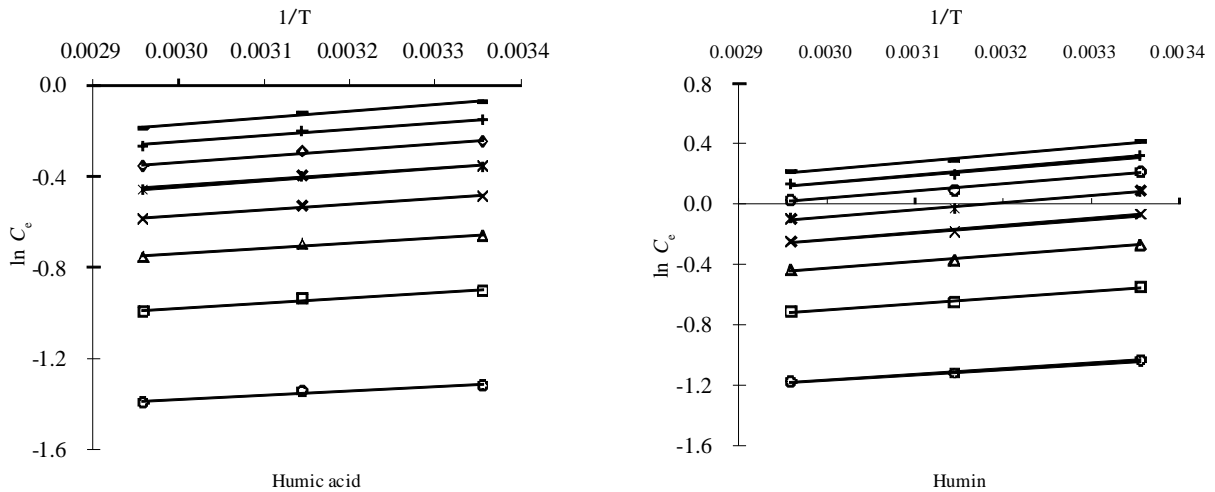
Fig. 4. Linear plot of ln C_e vs. 1/T for different amounts of Cu^{2+} adsorption on humic acid and humin, q_e=2 (○), 4 (□), 6 (△), 8 (×), 10 (*), 12 (◇), 14 (+), 16 (-) mg g^{-1}, from black soil
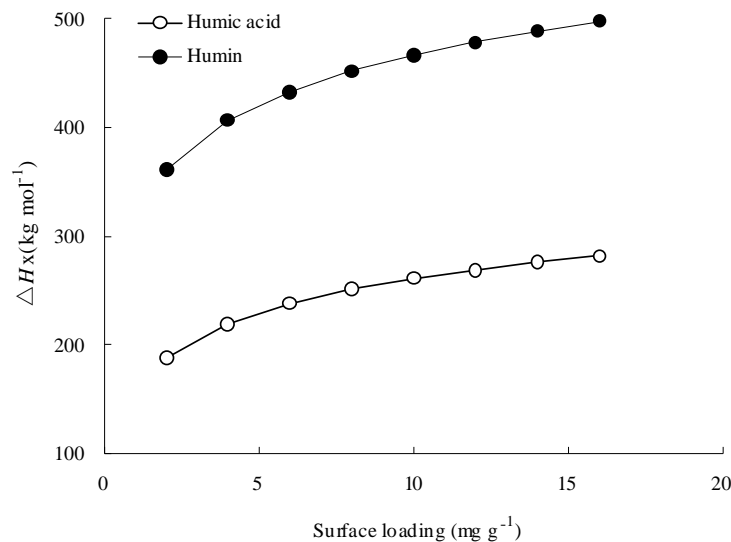
Fig. 5. Plot of isosteric heat of adsorption (ΔHx) against surface loading for the adsorption of Cu^{2+} on humic acid and humin from black soil

humic acids from peat soil and commercial Aldrich was spontaneous, endothermic and increasingly disordered process, in accordance with our results.

Compared with humic acid, the Δ$G°$ values of Cu^{2+} adsorption on humin were always more positive at each Cu^{2+} concentrations studied. It indicated that the adsorption of Cu^{2+} was more favorable on humic acid, in agreement with the larger values of the Freundlich constant n of humic acid. However, there was no consistent difference of the values of Δ$H°$ and Δ$S°$ between humic acid and humin.

The plots of ln C_e versus 1/T are plotted in Fig. 4, and the corresponding ΔH_x values are listed in Table

6. The plots of ln C_e versus 1/T were found to be linear with R^2 values greater than 0.943. The ΔH_x values ranged from 188.1 to 281.7 kJ mol^{-1} for humic acid and from 361.0 to 497.4 kJ mol^{-1}. The values of ΔH_x for physical and chemical adsorption are below 80 kJ mol^{-1} and between 80 and 400 kJ mol^{-1}, respectively (Chowdhurg *et al.*, 2011). Thus, our present results implied that the chemical adsorption involving ion exchange was the dominating mechanism. On the other hand, the variation of ΔH_x with surface loading (Fig. 5) showed that the ΔH_x values increased with the increase of q_e values, indicating that the adsorbents had energetically heterogeneous surfaces. The above variation in ΔH_x

Table 6. Isosteric heat of adsorption (ΔH_x) of Cu²⁺ on humic acid and humin from black soil

Samples	q_e (mg g⁻¹)	ΔH_x (kJ mol⁻¹)	R^2
Humic acid			
	2	188.1	0.943
	4	219.3	0.964
	6	237.5	0.972
	8	250.5	0.977
	10	260.5	0.980
	12	268.8	0.982
	14	275.7	0.984
	16	281.7	0.985
Humin			
	2	361.0	0.993
	4	406.5	0.989
	6	433.1	0.987
	8	451.9	0.985
	10	466.6	0.984
	12	478.5	0.983
	14	488.6	0.982
	16	497.4	0.982

values was usually due to the adsorbate-adsorbate interaction followed by the adsorbate-adsorbent interaction, and the possibility of having lateral interactions between adsorbed Cu²⁺ ions (Chowdhurg *et al.*, 2011; Srivastava *et al.*, 2007). The extent of the increase in ΔH_x values was larger for humic acid (49.8%) than for humin (37.8%), implying that humic acid had greater surface energy heterogeneity than humin. It agreed with the larger *n* values of humic acid with respect to humin in the Freundlich constant. In the study of Li *et al.* (2004), they indicated that the humic substance fractions with lower molecular weights, greater O/C atomic ratios, and higher contents of oxygen and lignin-derived aromatic structural units were more heterogeneous. Based on our present study, the O/C atomic ratio and the contents of oxygen and lignin-derived aromatic structural units of humic acid were all higher than that of humin. Meanwhile, the molecular weight of humic acid was generally considered lower than that of humin (Stevenson, 1994). It confirmed that the heterogeneity of humic acid was larger than that of humin. Thus, the difference in heterogeneity of adsorption surface of humic acid and humin could be due on their different chemical composition.

CONCLUSIONS

The chemical compositions of humin differed from those of corresponding humic acid. The former was more humified, aliphatic, hydrophobic, and less polar compared with the latter. The adsorption amounts of humin for Cu²⁺ were lower than that of humic acid.

The maximum adsorption capacities of Cu²⁺ on humin and humic acid were 227.3 and 243.9 mg g⁻¹ at 298 K, respectively. The adsorption data could be better described Freundlich equation with respect to equation. The increase in temperature had a positive effect on the sorption process. The adsorption of Cu²⁺ on humin and humic acid was a spontaneous, endothermic, and increasingly disordered process. Both humin and humic acid had energetically heterogeneous surfaces for the adsorption of Cu²⁺, and the surface energy heterogeneity of humic acid was greater than that of humin.

REFERENCES

Aiken, G. R., McKnight, D. M., Wershaw, R. L. and MacCarthy, P. (1985). Humic substances in soil, sediment, and water: Geochemistry, isolation, and characterization. New York: Wiley.

Alvarez-Puebla, R. A., Aroca, R. F., Valenzuela-Calahorro, C. and Garrido, J. J. (2006). Retention of cobalt on a humin

derived from brown coal. Journal of Hazardous Materials, **135 (1-3)**, 122-128.

Alvarez-Puebla, R. A., Valenzuela-Calahorro, C. and Garrido, J. J. (2004). Modeling the adsorption and precipitation of Cu(II) on humin. Journal of Colloid and Interface Science, **277 (1)**, 55-61.

Anirudhan, T. S. and Radhakrishnan, P. G. (2011). Thermodynamics of chromium(III) adsorption onto a cation exchanger derived from saw dust of Jack wood. Environmental Chemistry Letters, **9 (1)**, 121-125.

Chen, J.-S. and Chiu, C.-Y. (2003). Characterization of soil organic matter in different particle-size fractions in humid subalpine soils by CP/MAS ^{13}C NMR. Geoderma, **117 (1-2)**, 129-141.

Chowdhury, S., Mishra, R., Saha, P. and Kushwaha, P. (2011). Adsorption thermodynamics, kinetics and isosteric heat of adsorption of malachite green onto chemically modified rice husk. Desalination, **265 (1-3)**, 159-168.

Conte, P., Piccolo, A., van Lagen, B., Buurman, P. and de Jager, P. A. (1997). Quantitative differences in evaluating soil humic substances by liquid- and solid-state ^{13}C NMR spectroscopy. Geoderma, **80 (3-4)**, 339-352.

Contreras, C., de la Rosa, G., Peralta-Videa, J. R. and Gardea-Torresdey, J. L. (2006). Lead adsorption by silica-immobilized humin under flow and batch conditions: Assessment of flow rate and calcium and magnesium interference. Journal of Hazardous Materials, **133 (1-3)**, 79-84.

de la Rosa, G., Peralta-Videa, J. R. and Gardea-Torresdey, J. L. (2003). Utilization of ICP/OES for the determination of trace metal binding to different humic fractions. Journal of Hazardous Materials, **97 (1-3)**, 207-218.

Gardea-Torresdey, J. L., Tang, L. and Salvador, J. M. (1996). Copper adsorption by esterified and unesterified fractions of Sphagnum peat moss and its different humic substances. Journal of Hazardous Materials, **48 (1-3)**, 191-206.

Havelcová, M., Mizera, J., Sýkorová, I. and Pekaø, M. (2009). Sorption of metal ions on lignite and the derived humic substances. Journal of Hazardous Materials, **161 (1)**, 559-564.

Helal, A. A., Helal, Aly A., Salim, N. Z. and Khalifa, S. M. (2006). Sorption of radionuclides on peat humin. Journal of. Radioanalytical and Nuclear Chemistry, **267 (2)**, 363-368.

Helal, A. A., Helal, Aly A., Salim, N. Z. and Khalifa, S. M. (2006). Effect of some environmental ligands on the sorption of radionuclides by peat humin. Journal of. Radioanalytical and Nuclear Chemistry, **267 (2)**, 369-375.

Helal, A. A., Imam, D. M. and Aly, H. F. (1998). Interaction of Cs^+, Sr^{2+} and Gd^{3+} with humin. Journal of. Radioanalytical and Nuclear Chemistry, **237 (1-2)**, 7-11.

Krull, E. S., Skjemstad, J. O. and Baldock, J. A. (2004). Functions of soil organic matter and the effect on soil properties. GRDC report, Project CSO 00029.

Lao, J. C. (1988). Handbook of soil agro-chemistry analysis. Beijing: Agriculture Press.

Li, L., Zhao, Z., Huang, W., Peng, P., Sheng, G. and Fu, J. (2004). Characterization of humic acids fractionated by ultrafiltration. Organic Geochemistry, **35 (9)**, 1025-1037.

Li, X., Zhou, Q., Wei, S., Ren, W. and Sun, X. (2011). Adsorption and desorption of carbendazim and cadmium in typical soils in northeastern China as affected by temperature. Geoderma, **160 (3-4)**, 347-354.

Li, Y., Yue, Q., Gao, B., Li, Q. and Li, C. (2008). Adsorption thermodynamic and kinetic studies of dissolved chromium onto humic acids. Colloids and Surfaces B: Biointerfaces, **65 (1)**, 25-29.

Mahmoodi, N. M., Hayati, B., Arami, M. and Lan, C. (2011). Adsorption of textile dyes on Pine Cone from colored wastewater: Kinetic, equilibrium and thermodynamic studies. Desalination, **268 (1-3)**, 117-125.

Mathers, N. J. and Xu, Z. (2003). Solid-state ^{13}C NMR spectroscopy: characterization of soil organic matter under two contrasting residue management regimes in a 2-year-old pine plantation of subtropical Australia. Geoderma, **114 (1-2)**, 19-31.

Perminova, I. V., Hatfield, K. and Hertkorn, N. (2005). Use of humic substances to remediate polluted environments: From theory to practice. Dordrecht: Springer.

Prado, A. G. S. and Airoldi, C. (2003). Humic acid-divalent cation interactions. Thermochimica Acta, **405 (2)**, 287-292.

Rice, J. A. (2001). Humin. Soil Science, **166 (11)**, 848-857.

Rigol, A., Vidal, M. and Rauret, G. (1998). Competition of organic and mineral phases in radiocesium partitioning in organic soils of Scotland and the area near Chernobyl. Environmental Science and Technology, **32 (5)**, 663-669.

Schnitzer, M. (1999). A lifetime perspective on the chemistry of soil organic matter. Advances in Agronomy, **68**, 1-58.

Sheng, G., Wang, S., Hu, J., Lu, Y., Li, J., Dong, Y. and Wang, X. (2009). Adsorption of Pb(II) on diatomite as affected via aqueous solution chemistry and temperature. Colloids and Surfaces A: Physicochemical and Engineering Aspects, **339 (1-3)**, 159-166.

Simpson, A. J., McNally, D. J. and Simpson, M. J. (2011). NMR spectroscopy in environmental research: From molecular interactions to global processes. Progress in Nuclear Magnetic Resonance Spectroscopy, **58 (3)**,97-175.

Srivastava, V. C., Mall, I. D. and Mishra, I. M. (2007). Adsorption thermodynamics and isosteric heat of adsorption of toxic metal ions onto bagasse fly ash (BFA) and rice husk ash (RHA). Chemical Engineering Journal, **132 (1-3)**, 267-278.

Stevenson, F. J. (1994). Humic chemistry: Genesis, composition, reactions, second editor. New York: Wiley & Sons.

Xing, B., Liu, J., Liu, X. and Han, X. (2005). Extraction and characterization of humic acids and humin fractions from a black soil of China. Pedosphere, **15 (1)**, 1-8.

Zhang, J., Dai, J., Wang, R., Li, F. and Wang W. (2009). Adsorption and desorption of divalent mercury (Hg^{2+}) on humic acids and fulvic acids extracted from typical soils in China. Colloids and Surfaces A: Physicochemical and Engineering Aspects, **335 (1-3)**, 194-201.

Zhang, J., Dou, S. and Song, X. (2009). Effect of long-term combined nitrogen and phosphorus fertilizer application on ^{13}C CPMAS NMR spectra of humin in a Typic Hapludoll of northeast China. European Journal of Soil Science, **60 (6)**, 966-973.

Zhang, J., Hu, F., Li, H., Gao, Q., Song, X., Ke, X. and Wang, L. (2011a). Effects of earthworm activity on humus composition and humic acid characteristics of soil in a maize residue amended rice-wheat rotation agroecosystem. Applied Soil Ecology, **51**, 1-8.

Zhang, J., Wang, S., Wang, Q., Wang, N., Li, C. and Wang, L. (2013). First determination of Cu adsorption on soil humin. Environmental Chemistry Letters, **11 (1)**, 41-46.

Zhang, Y., Du, J., Zhang, F., Yu, Y. and Zhang, J. (2011b). Chemical characterization of humic substances isolated from mangrove swamp sediments: The Qinglan area of Hainan Island, China. Estuarine Coastal and Shelf Science, **93 (3)**, 220-227.